geographies

MDPI

Article

A Comprehensive Assessment of Rangeland Suitability for Grazing Using Time-Series Remote Sensing and Field Data: A Case Study of a Steppe Reserve in Jordan

Rana N. Jawarneh [1,*], Zeyad Makhamreh [2], Nizar Obeidat [3] and Ahmed Al-Taani [4]

[1] Applied Geography and GIS Program, Department of Humanities, Qatar University, Doha P.O. Box 2713, Qatar
[2] Department of Geography, Faculty of Arts, Jordan University, Amman 11942, Jordan; z.makhamreh@ju.edu.jo
[3] National Agriculture Research Center (NARC), Balqa 19381, Jordan; nizar.obeidat@narc.gov.jo
[4] Department of Earth and Environmental Sciences, Faculty of Science, Yarmouk University, Irbid 21510, Jordan; taaniun@yu.edu.jo
* Correspondence: rnjawarneh@qu.edu.qa

Abstract

This study employs an integrated framework that combines field-based measurements, remote sensing, and Geographic Information Systems (GISs) to monitor vegetation dynamics and assess the suitability of a steppe range reserve for livestock grazing. Forty-three surface and subsurface soil samples were collected in April and November 2021 to capture seasonal variations. Above-ground biomass (AGB) measurements were recorded at five sampling locations across the reserve. Six Sentinel-2 satellite imageries, acquired around mid-March 2016–2021, were processed to derive time-series Normalized Difference Vegetation Index (NDVI) data, capturing temporal shifts in vegetation cover and density. The GIS-based Multi-Criteria Decision Analysis (MCDA) was employed to model the suitability of the reserve for livestock grazing. The results showed higher salinity, total dissolved solids (TDSs), and nitrate (NO_3) values in April. However, the percentage of organic matter increased from approximately 7% in April to over 15% in November. The dry forage productivity ranged from 111 to 964 kg/ha/year. On average, the reserve's dry yield was 395 kg/ha/year, suggesting moderate productivity typical of steppe rangelands in this region. The time-series NDVI analyses showed significant fluctuations in vegetation cover, with lower NDVI values prevailing in 2016 and 2018, and higher values estimated in 2019 and 2020. The grazing suitability analysis showed that 13.8% of the range reserve was highly suitable, while 24.4% was moderately suitable. These findings underscore the importance of tailoring grazing practices to enhance forage availability and ecological resilience in steppe rangelands. By integrating satellite-derived metrics with in situ vegetation and soil measurements, this study provides a replicable methodological framework for assessing and monitoring rangelands in semi-arid regions.

Keywords: vegetation dynamics; rangelands monitoring; soil attributes; GIS-MCDA; semi-arid grassland; Jordan

check for updates

Academic Editors: Pere Serra and Jorge Rocha

Received: 19 August 2025
Revised: 29 September 2025
Accepted: 28 October 2025
Published: 1 November 2025

Citation: Jawarneh, R.N.; Makhamreh, Z.; Obeidat, N.; Al-Taani, A. A Comprehensive Assessment of Rangeland Suitability for Grazing Using Time-Series Remote Sensing and Field Data: A Case Study of a Steppe Reserve in Jordan. *Geographies* **2025**, *5*, 63. https://doi.org/10.3390/geographies5040063

Copyright: © 2025 by the authors. Licensee MDPI, Basel, Switzerland. This article is an open access article distributed under the terms and conditions of the Creative Commons Attribution (CC BY) license (https://creativecommons.org/licenses/by/4.0/).

1. Introduction

Rangelands represent one of the Earth's most extensive land cover types, spanning approximately 79 million km^2 and comprising approximately 24% of the planet's terrestrial surface. Notably, 43% of these rangelands are situated in arid or semi-arid regions [1–4].

Rangelands provide vital ecosystem services and sequester nearly one-third of the terrestrial carbon. They account for 91% of the world's grazing lands and support approximately 50% of the global livestock population [5–7]. Nevertheless, nearly half of the world's rangelands are degraded due to overgrazing, unsustainable land-use practices, and agricultural encroachment [8,9]. In the Mediterranean region, where rangelands cover 80% of the land area, nearly 23% of those rangelands have been desertified [10]. The escalating demand for forage exceeds the potential productivity of the grazing resources [11]. In the Middle East, rangelands dominate the arid and semi-arid zones. They are locally known as steppe (Badia) and cover approximately 510 million hectares in the Arab countries, of which 51 million are located in the Mashreq region [6,12]. Over 90% of Jordan's landmass is classified as arid and semi-arid, with 81% of this area locally known as Badia, playing a critical role in sustaining pastoralist communities and supporting extensive livestock production systems [13–15]. The Badia rangelands have made a substantial contribution to the domestic forage supply, providing year-round natural grazing for sheep and other range-dependent livestock [16]. The steppe region, in particular, which consists of 12% of the country's area, represents the semi-arid transitional zone between the sub-humid and the arid zone, possessing abundant natural resources, such as mineral deposits, surface and groundwater, renewable grazing lands, and agricultural land suitable for crop cultivation and livestock production [12,17,18].

However, forage yields in these areas have sharply declined due to overgrazing, inadequate land management, and the increasing impact of climate change [11,14,19]. It was estimated that the palatable dry biomass production in Jordanian rangelands decreased by approximately half between the 1990s and 2010, severely impacting the livestock feed supply system [20,21]. As a result, the Jordanian Ministry of Agriculture and the Department of Protected Reserves have taken measures to protect these natural pastures. Since 2001, strategies have been implemented to resolve economic, social, and environmental challenges, including unclear pastureland ownership, rising livestock numbers, and ineffective pastureland regulations [16].

Although Jordan's Ministry of Agriculture has established 35 rangeland reserves and has developed annual protection plans, maintaining sustainability in these reserves remains challenging, particularly in arid and semi-arid regions [22]. Managed grazing has been widely recognized as a sustainable practice for maintaining productive and healthy rangeland ecosystems, covering more than 25% of the global land surface and surpassing all other land-use types in terms of geographical extent [7]. In Jordan, protection strategies have also shown measurable ecological benefits. For instance, Al-Satari et al. [23] demonstrated that community-based rangeland protection improved vegetation recovery and livestock sustainability, while Alokour et al. [24] reported that protection measures in the Shoubak region significantly enhanced the productivity of native vegetation. These findings reinforce the importance of combining protection with managed grazing to sustain rangeland ecosystems in semi-arid environments. Therefore, research on the suitability and sustainability of managed grazing practices and management policies continues to identify high-quality grazing zones and restore low-quality zones. Several methods have been implemented to estimate forage production in these protected areas and assess suitability for livestock grazing, such as traditional clip-and-weigh techniques. Nevertheless, these methods are labor-intensive and spatially restrictive [25,26]. Advances in remote sensing, however, have enabled scalable vegetation monitoring through long-term vegetation-derived indices, such as NDVI and Modified Soil-Adjusted Vegetation Index (MSAVI) [27]. Additional parameters are needed to capture seasonal variations [28].

Research efforts in Jordan have explored various strategies for restoring degraded rangelands, including introducing drought-tolerant grasses and native shrubs [29], opti-

mizing grazing management to reduce livestock feeding costs [30], enhancing semi-arid ecosystem resilience through assessing long-term controlled grazing [31], and understanding the socioeconomic factors influencing rangeland policy effectiveness [32]. Recent studies have also examined how population growth and the influx of Syrian refugees have exacerbated rangeland degradation, using Landsat 8 remote sensing data [33]. Moreover, protected rangeland areas have substantially improved vegetation productivity, biomass yield, and sustainable livestock stocking rates [24]. The COVID-19 lockdown was a unique natural experiment, highlighting how reduced human activities and controlled grazing allowed vegetation recovery in Jordan's Badia region [34]. Water harvesting techniques have also shown promising results in mitigating soil erosion and rehabilitating degraded ecosystems in Badia [6]. Despite these interventions, a significant imbalance persists between livestock populations and available rangeland resources, characterized by rapid, potentially irreversible land degradation, rising livestock numbers, declining livestock productivity, and deteriorating conditions for poorer pastoral communities. Addressing this imbalance remains crucial for achieving sustainable grazing practices and ensuring the long-term Suitability of Jordan's rangeland reserves.

Monitoring long-term vegetation biomass in arid and semi-arid zones by remote sensing has been proven to aid natural resource management [35]. In combination with GIS modeling techniques, remote sensing technologies offer powerful tools for rangeland assessment and grazing suitability analysis [36–39]. GIS-based Multi-Criteria Decision Analysis (MCDA) provides a comprehensive approach for integrating environmental and socioeconomic factors into rangeland suitability assessments [40,41]. MCDA has proven effective in predicting land-use scenarios, assessing soil potential, and identifying optimal grazing zones [42,43]. As a case study conducted in Jordan's highly vulnerable steppe ecosystems and within a range reserve, this study integrates remote sensing data, field-based vegetation biomass measurements, soil analysis, and GIS-based MCDA to develop the first livestock suitability maps for Al-Khanasri Reserve.

The primary goal of this study is to develop a comprehensive, spatially informed framework for assessing rangeland productivity and grazing suitability in the Al-Khanasri Reserve, Jordan. Specifically, the study aims to: (1) monitor spatiotemporal dynamics of vegetation cover using time-series remote sensing data, (2) evaluate soil and vegetation attributes in relation to forage availability and ecological resilience, and (3) generate GIS-based suitability maps that classify areas according to their potential for sustainable livestock grazing. Through this integrated approach, the study provides a timely and methodologically rigorous response to the challenges of estimating forage production and identifying suitable grazing zones amid land degradation, overgrazing, climate variability, and unsustainable land use. By mapping current land conditions and informing the strategic management of rangeland reserves within the marginal steppe ecoregion, the study offers actionable insights to enhance ecological resilience and pastoral livelihoods. More broadly, it supports SDG 15 (Life on Land) by identifying suitable zones for livestock production, contributes to food security and resilient rural livelihoods under SDG 2 (Zero Hunger), and promotes SDG 12 (Responsible Consumption and Production) through the application of geospatial analysis to optimize resource use and improve land governance [44].

2. Materials and Methods

2.1. Study Area

Al-Khanasri reserve is located within the northern steppe rangeland of Jordan [45] (Figure 1) and was first established in 1946, covering a total area of 455 hectares. It is protected year-round, with grazing permitted only during spring and autumn. Grazing is allowed for three months in the spring (April, May, and June) and for one month in November. The number of sheep introduced into the reserve depends on the availability of forage and on the appropriate stocking rate to ensure sustainable pasture use. The study area is part of the semi-arid plain region in northern Jordan, characterized by dry, hot summers (average maximum temperatures of 30–35 °C) and mild to cold winters [33,46]. The annual rainfall ranges between 200 and 250 mm. As part of the Northern Highlands Dissected Limestone, the reserve spans a hilly terrain characterized by steep slopes and undulating topography, with altitudes ranging from 648 to 857 m above sea level. The dominant soils are Inceptisols, specifically the subgroups Xerochrept and Calcixerollic. These are moderately developed and characterized by silty-textured soils with a high carbonate content and low organic matter content. Rainfed agriculture, rangelands, and sparsely vegetated areas dominate the surrounding land cover.

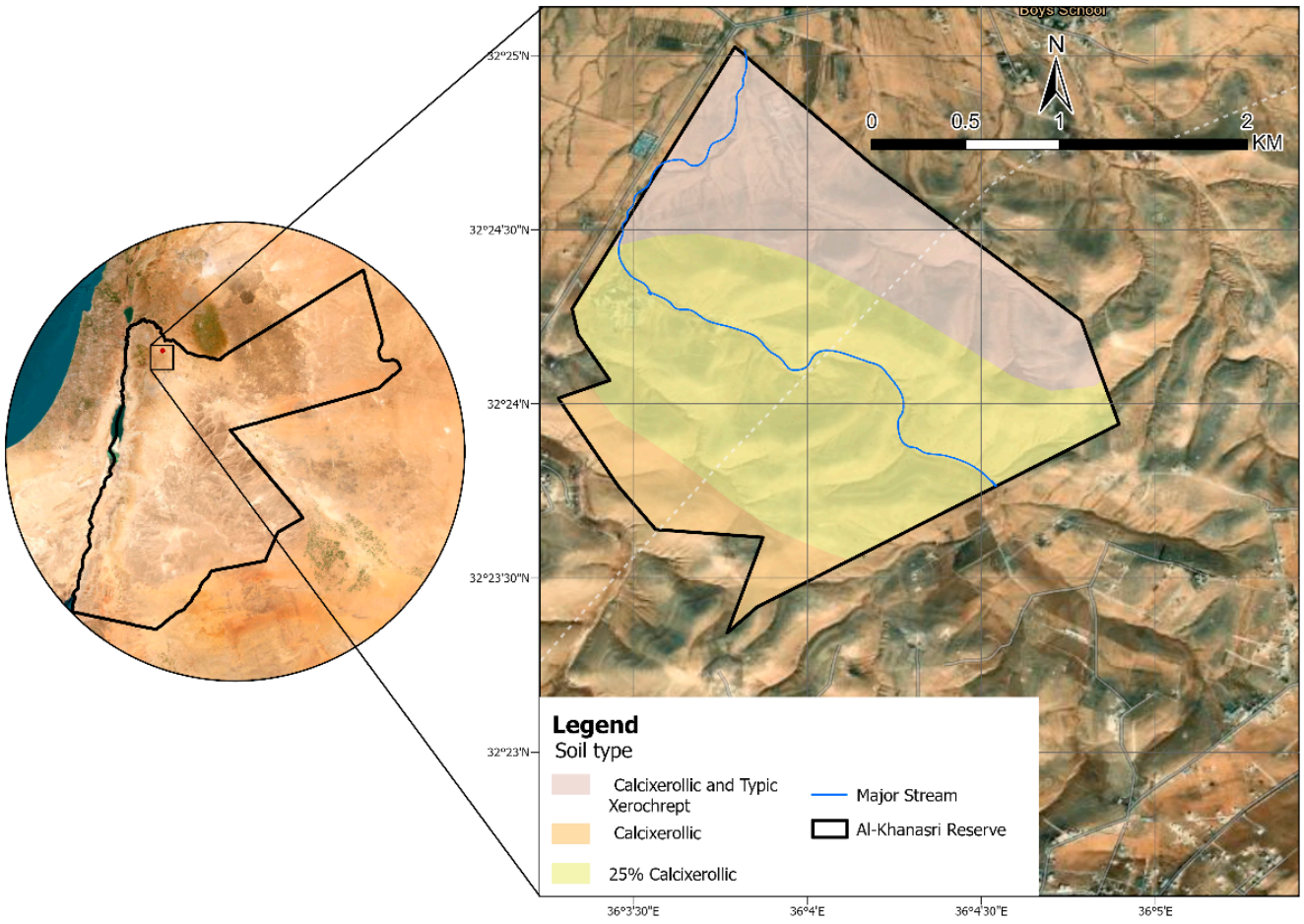


Figure 1. Location of the study area.

2.2. Data Sources

A comprehensive dataset from multiple sources was utilized in this study (Table 1). The soil attributes were measured in 43 surface and subsurface samples collected from the range reserve in April and November 2021. The above-ground biomass information was obtained from 250 samples collected across the range reserve in April 2022 to estimate the available forage. Vegetation density maps were derived from 10 m resolution Sentienal-2 images using the Normalized Difference Vegetation Index (NDVI). These Sentinel-2 Multi-Spectral Instrument (MSI) imageries were retrieved from the Copernicus Open Access Hub at "https://dataspace.copernicus.eu/data-collections/copernicus-sentinel-data/sentinel-2 (accessed on 20 November 2023)" for the years 2016, 2017, 2018, 2019, 2020, and 2021, with all scenes acquired around mid-March to capture the peak of vegetation growth. Biodiversity data to identify dominant species were collected through field surveys carried out in April 2022, coinciding with the peak of the growing season. Topographic characteristics of the range reserve, particularly the slope aspect, were delineated from the Digital Terrain Model (DEM) at 10 m resolution obtained from the Royal Jordanian Geographical Center (RJGC). The major streams in the range reserve were derived from the DEM using the Hydrology toolset in ArcPro 3.3, and the Euclidean distance tool was used to derive the water accessibility map [47].

Table 1. Variables examined in the study, grouped by major characteristics, with corresponding data sources. NDVI refers to Normalized Difference Vegetation Index; DEM refers to Digital Elevation Model; and MSI refers to Multispectral Instrument.

Major Characteristics	Name of the Variable	Source
Soil attributes	Potential of Hydrogen (pH); Total Dissolved Solids (TDS); Electrical Conductivity (EC); Salinity; Moisture content; Calcium Carbonate ($CaCO_3$); Fluoride (F); Chloride (Cl); Nitrate (NO_3); Phosphate (PO_4); Sulfate (SO_4)	Primary surface and sub-surface soil data were collected during field surveys from 43 sites in the reserves in the Spring and Fall of 2021 (Laboratory Test).
Biomass	Biomass measurements	250 plant samples were collected from 5 locations within the reserve using the Quadrats Transect method and the Clip-and-weigh method. Oven-dried in the laboratory to calculate forage dry biomass.
	Plants species	29 samples collected across the reserves using the Quadrats Transect method.
	(NDVI)	derived from Sentinel-2A MSI (2016–2021) Satellite imageries at 10 m resolution. Retrieved from Copernicus Open Access Hub at https://dataspace.copernicus.eu/data-collections/copernicus-sentinel-data/sentinel-2 (accessed on 20 November 2023)
Topography and use	Land use map	Manually digitized from 2021 Sentinel-2A MSI image.
	Slope (%) and aspect	Derived from 10 m DEM obtained from Royal Jordanian Geographical Center.
	Water accessibility	Derived from 10 m DEM using Hydrology toolset and Ecludian distance.

2.3. Methods

Our methodology combined Sentinel-2 imagery, DEM data, field surveys, and laboratory analyses to evaluate the suitability of the Al-Khanasri reserve for livestock grazing. Remote sensing provided information on land cover, NDVI, vegetation density, and terrain variables, while field data supplied details on biomass, soil, and biodiversity. These inputs were transformed into suitability layers and integrated through the Analytical Hierarchy Process (AHP) and weighted overlay to generate the final grazing suitability map (Figure 2).

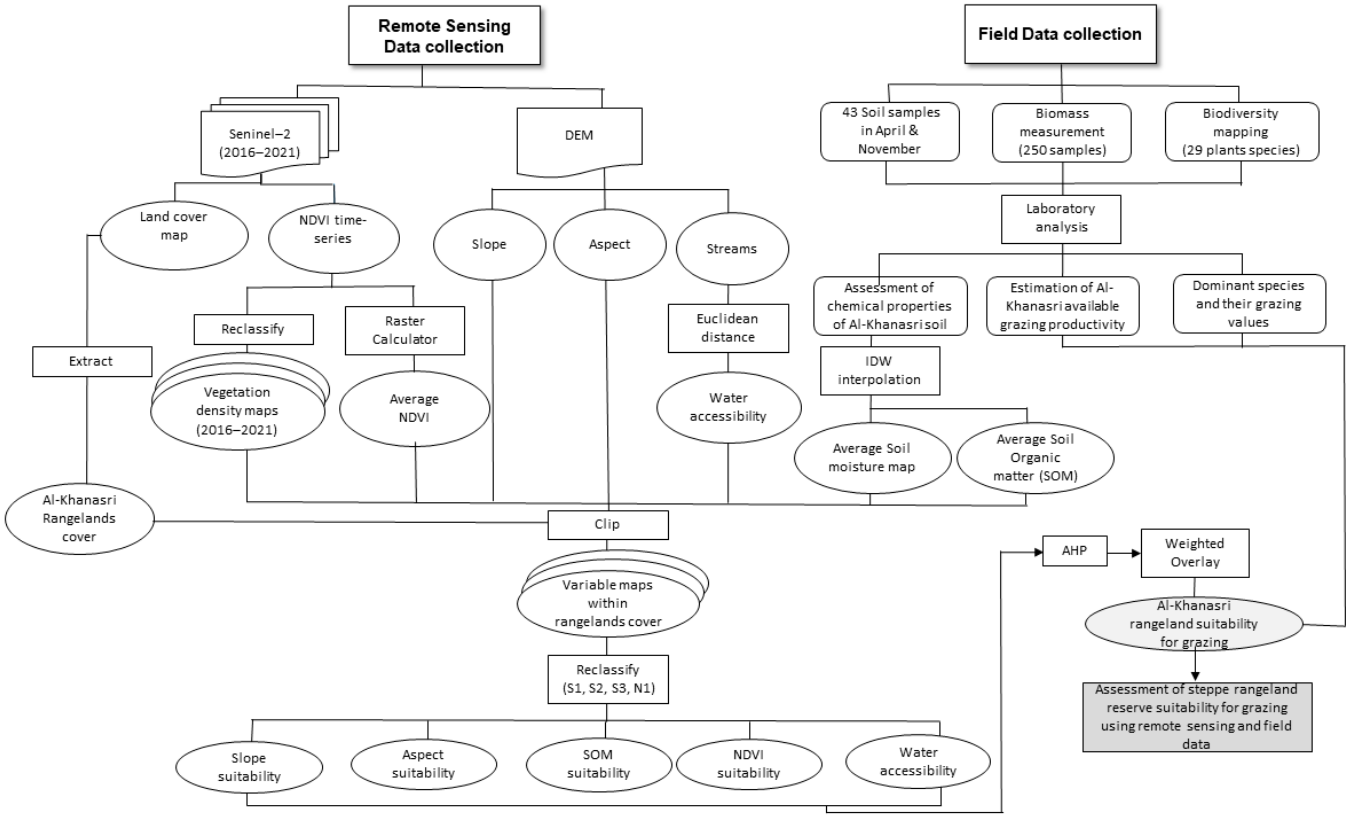


Figure 2. Flowchart of the methodology.

2.3.1. Soil Sampling and Analysis

A total of 43 soil samples were systematically collected across the reserve on 5 April 2021 and 29 November 2021. In the initial sampling stage, conducted at the end of the growing season with no preceding rainfall, 20 samples were collected, including 12 surface samples and 11 subsurface samples. In the second sampling stage, conducted at the beginning of the rainy season, 20 soil samples were collected, including 13 surface samples and seven subsurface samples. Sampling was conducted across three depth intervals—0–20 cm, 20–40 cm, and 40–60 cm—based on the reserve's topography and soil profile.

Soil samples were sealed in the field and transported to the laboratory for physicochemical analysis. Gravimetric moisture content was determined by the oven-drying (thermogravimetric) method [48] ~2.0 g of fresh soil was weighed into a clean, dry crucible, dried at 105 °C for 3–5 h to constant mass, reweighed, and moisture (%) computed as follows:

$$\text{Soil Moisture Content } (\%) = \frac{(Frsh\ weight - Dry\ weight(105\ ^\circ\text{C}))}{Fresh\ Weight} \times 100 \quad (1)$$

For aqueous measurements, air-dried soils were extracted with deionized water. For rapid pH and EC determinations, suspensions at a 1:5 soil/solution ratio were shaken for

90 min, centrifuged, and the supernatant was filtered through a 0.45 µm membrane prior to analysis [49]. For a comprehensive solution chemistry, 10 g soil was mixed with 50 mL distilled water in centrifuge tubes, shaken for 24 h, and centrifuged at 4500 rpm for 20 min. The supernatant was used for pH (EcoScan Handheld Series, by Eutech Instruments Pte Ltd., Singapore); for TDS, EC, and salinity (Sension 5, HACH, Singapore) per [1]; and for anions (Cl^-, $NO_2{}^-$, $NO_3{}^-$, $SO_4{}^{2-}$, $PO_4{}^{3-}$) by ion chromatography (DIONEX ICS-1600, Thermo Scientific, Waltham, MA, USA) according to [50].

Total organic matter was quantified by loss-on-ignition. Approximately 2.0 g of soil pre-dried at 105 °C was ashed at 550 °C for 3–5 h in a muffle furnace, and organic matter (%) was calculated as follows [51,52]:

$$\text{Organic matter} = \frac{Weight\ (105\ ^\circ\text{C}) - Weight\ (550\ ^\circ\text{C})}{Weight\ (105\ ^\circ\text{C})} \times 100 \quad (2)$$

Carbonate content was determined using a calcimeter with pure $CaCO_3$ as the standard [51]. A 0.5 g soil subsample was reacted with 10 mL of 10% HCl; the evolved CO_2 was measured, and $CaCO_3$ (%) computed as follows:

$$CaCO_3\% = \frac{CO_2\ from\ sample}{CO_2\ from\ standard} \times 100 \quad (3)$$

2.3.2. Land Use Mapping

Because this range reserve is also a research station managed by the National Agriculture Research Center (NARC), it has mixed uses of the land. We manually digitized the land uses from the 2021 Sentinel-2 satellite imagery, delineating four land uses: built-up areas, cultivated areas (primarily barley), a protected military site, and natural rangeland. However, for this research, field surveys and analyses were carried out only within the natural rangelands. The map was also verified during multiple visits to the reserve.

2.3.3. Available Forage Biomass Estimation

Above-ground biomass was estimated using 250 quadrats at five sampling sites within the reserve, using the Quadrats Transect method with a plot size of 1 m^2 and 120 m transect length with 5 m quadrat intervals (Figure 3). These sites were selected for their physiographic homogeneity, and samples were collected in April 2022 to ensure accurate estimations. The Clip-and-Weigh Method was used to estimate the available forage. All vegetation, both palatable and non-palatable, was clipped at ground level [53]. The harvested material was then sorted to remove non-palatable species, and only the palatable portion was dried in an oven to determine its dry weight. This process provides an accurate estimate of the forage truly accessible to grazing animals, offering a direct and objective assessment of forage availability at the time of sampling. The samples were labeled in bags from each plot separately and transferred to the laboratory, where they were oven-dried at a temperature of 60–80 °C for 48–72 h to determine the dry weight in kilograms per square meter using the following equation:

$$\text{Biomass}\ (\text{kg}/\text{m}^2) = \frac{Dry\ weight\ (\text{kg})}{Plot\ Area\ (\text{m}^2)} \quad (4)$$

Then, we multiplied the biomass per square meter by 10,000 to convert to hectares.

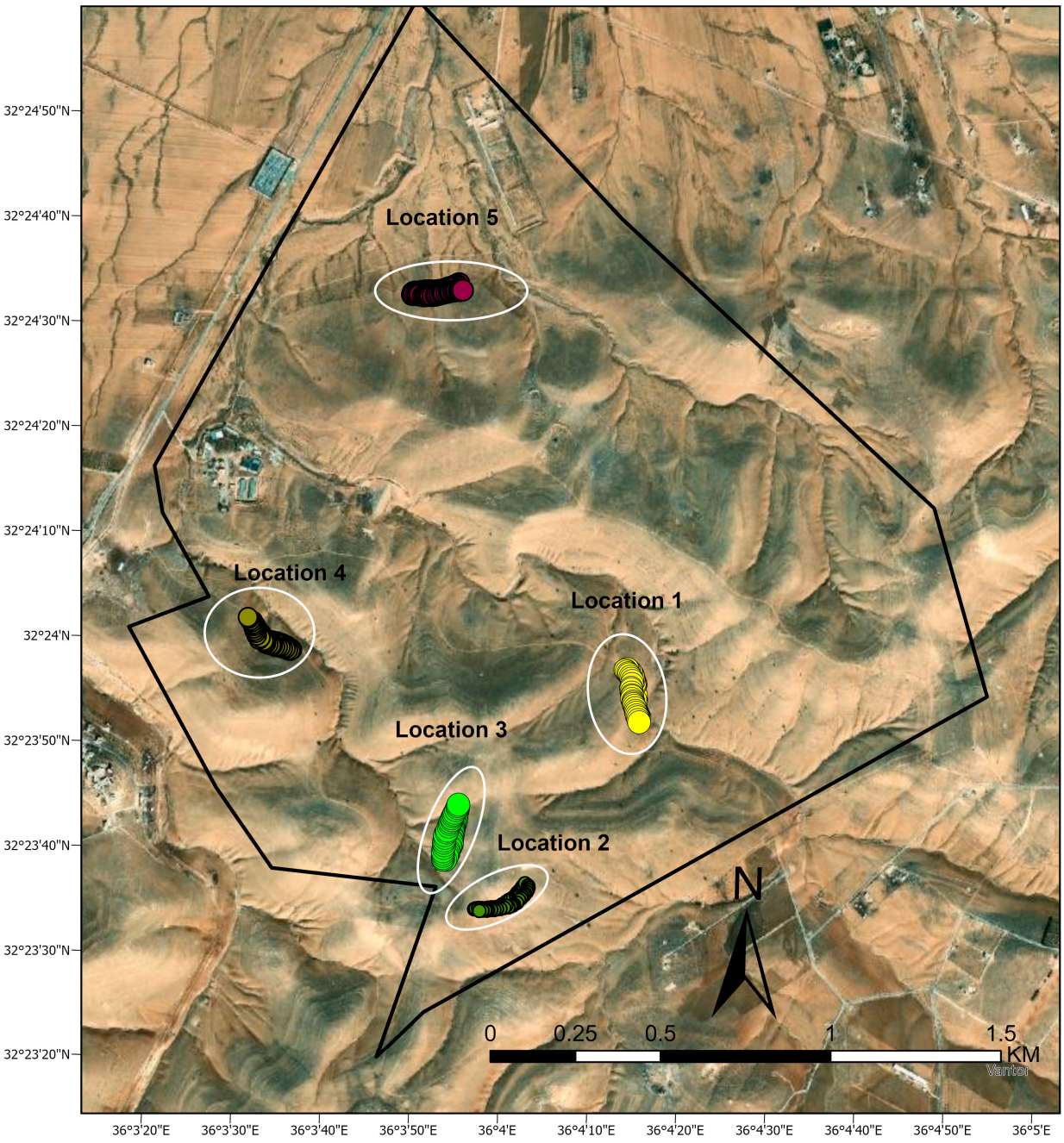


Figure 3. Spatial distribution of sampling sites within the Al-Khanasri Reserve. The map illustrates five designated sampling locations, each comprising multiple transects with small circles representing the 250 quadrats (1 m^2) used to measure available forage biomass.

2.3.4. Remote Sensing-Based Vegetation Density Analysis

The six Sentinel-2 scenes from 2016, 2017, 2018, 2019, 2020, and 2021 were used to derive the NDVI time series. The acquisition dates ranged from 11 March to 16 March, reflecting the growth peak in the reserve and ensuring spatial consistency and coverage of the main phenological stages of vegetation. Sentinel-2 is an advanced sensor designed to capture high-resolution optical imagery across 13 spectral bands, spanning the visible, near-infrared (NIR), and shortwave infrared (SWIR) regions of the electromagnetic spectrum [54,55]. With a spatial resolution of 10 m for NDVI calculations, Sentinel-2 MSI provides detailed observations suitable for a wide range of applications, including agriculture, forestry, land cover classification, and disaster management. The NDVI has proven to be an effective tool for estimating vegetation biomass and assessing spatial variability

in productive areas, particularly in semi-arid rangelands [56]. The Sen2Cor algorithm was used within the Sentinel Application Platform environment (SNAP) to perform atmospheric corrections and provide bottom-of-atmosphere reflectance data [57]. The NDVI was calculated using the spectral bands 4 (red) and 8 (NIR) using the following equation:

$$\text{NDVI} = \frac{(\text{B8} - \text{B4})}{(\text{B8} + \text{B4})} \quad (5)$$

where B_8 is the band number 8 (near-infrared reflectance) and B_4 is the band number 4 (reflectance corresponding to red).

2.3.5. Plants Biodiversity in Al-Khanasri

The dominant species, their families, life spans, and coverage rates were identified in four field surveys conducted in April 2022. These surveys were strategically scheduled during the peak growing season to ensure accurate and comprehensive observations. Plant samples were systematically collected through walking transects, allowing for a thorough assessment of the plant communities across the study area.

2.3.6. GIS-Based Multi-Criteria Decision Analysis (MCDA) Grazing Suitability

We used several factors in the MCDA suitability analysis. Soil properties, including average organic matter (SOM) and moisture content, were selected as SOM is fundamental for maintaining soil health and improving soil structure and water-holding capacity. Soil moisture is equally crucial, providing plants with the water required for vital physiological processes such as photosynthesis, nutrient uptake, and transpiration. The soil attributes were averaged from the two collection periods and then interpolated using Inverse Distance Weight (IDW) method in ArcGISPro v 3.4. Because terrain topography significantly influences spatial heterogeneity and the distribution of essential resources such as moisture and nutrients [8,58,59], the slope (%) factor was included and derived from the DEM using the surface analysis toolset in ArcGIS Pro v 3.4 [47]. The aspect factor was also included in the model, as it affects soil moisture and vegetation growth. Slopes with a north-facing aspect often retain more moisture due to reduced solar radiation, fostering conditions favorable for nutrient accumulation and vegetation growth [60]. On the contrary, south-facing slopes may experience higher evaporation rates and reduced moisture availability, resulting in less favorable conditions for biomass production [61]. Water resource accessibility was another factor considered, and it was mapped in terms of distance from the local Wadis. Vegetation density was calculated as the average of the NDVI time series.

Each of the above-mentioned grazing suitability factors was rated, reclassified, and standardized into four suitability classes: highly suitable (S1), moderately suitable (S2), marginally suitable (S3), and not suitable (N1), as outlined in Table 2. This classification adheres to the guidelines provided by the Food and Agriculture Organization [62]. The weights of each factor were determined using the Analytic Hierarchy Process (AHP) [63,64]. The AHP method is the most widely used as it incorporates stakeholder judgments to establish the relative importance of each criterion on a scale from 1 to 9. Criteria weights were derived through the pairwise comparison matrices constructed within TerrSet's Analytic Hierarchy Process (AHP) module [64]. These weights were integrated into the Multi-Criteria Evaluation (MCE) module using the Weighted Linear Combination (WLC) decision rule to generate the final suitability map. In this research, we extensively engaged multiple stakeholders throughout the project's implementation period to capture their insights on the relative importance of the various criteria.

Table 2. Rangeland evaluation criteria and their suitability classes for sheep and goats. Suitability classes are defined as: highly suitable (S1), moderately suitable (S2), marginally suitable (S3), and not suitable (N1).

Criteria	S1	S2	S3	N1
Av. Soil Organic Matter	>5	3–5	1–3	<1
Av. Soil moisture content (%)	20–30	10–20	5–10	<5
Slope (%)	0–16	16–35	35–50	>50
Aspect	N, NE	E, SE	W, NW	S, SW
Av. NDVI-based vegetation density	>0.4	0.4–0.3	0.3–0.1	<0.1
Water accessibility (M)	<1	1–3	3–5	>5

3. Results

3.1. Soil Characteristics

The soils of the Al-Khanasri reserve were classified mainly as Aridisols and Entisols, both typical of semi-arid rangelands with steep topography and carbonate-rich geology. These soils are characterized by shallow profiles, limited organic matter, and variable fertility, which strongly influence rangeland productivity. The carbonate-dominated parent material provides a buffering effect, maintaining soils in slightly alkaline conditions throughout the year. This was confirmed by the pH values measured in April (7.56 ± 0.30) and November (7.53 ± 0.17) (Table 3), which were statistically indistinguishable (p = 0.688). Such stability is ecologically important because pH strongly regulates the solubility of nutrients and microbial activity. The persistence of slightly alkaline conditions ensures the continued availability of most macronutrients while preventing harmful acidification.

Table 3. Statistical comparison of soil parameters for samples collected in April and November 2021.

Parameter	n (Pairs)	April Mean ± SD	November Mean ± SD	95% CI (April)	95% CI (Nov.)	% Change	Test Used	*p*-Value	Cohen's d
Salinity (%)	10	0.300 ± 0.133	0.150 ± 0.053	0.205–0.395	0.112–0.188	−50.0%	Paired *t*-test	0.0067	−1.11
EC (µS/cm)	10	704.1 ± 304.0	246.0 ± 58.9	486.6–921.6	203.9–288.1	−65.0%	Paired *t*-test	0.0008	−1.55
TDS (mg/kg)	10	1544.8 ± 681.8	707.7 ± 168.5	1057.0–2032.5	587.1–828.2	−54.2%	Paired *t*-test	0.0031	−1.26
pH	10	7.56 ± 0.30	7.53 ± 0.17	7.34–7.77	7.41–7.65	−0.4%	Paired *t*-test	0.688	−0.09
$CaCO_3$ (%)	15	27.50 ± 13.68	20.28 ± 9.19	19.9–35.1	15.2–25.4	−26.3%	Wilcoxon signed-rank	0.151	−0.38
Moisture (%)	13	3.88 ± 1.41	9.42 ± 2.52	3.06–4.70	7.95–10.89	142.70%	Mann–Whitney U	0.037	NA
Organic Content (%)	13	7.11 ± 1.68	15.26 ± 1.72	6.13–8.09	14.24–16.28	114.70%	*t*-test	0.78	−0.12

The carbonate content showed a moderate seasonal decline, from 27.5 ± 13.7% in April to 20.3 ± 9.2% in November, representing a 26% reduction (Table 3). However, this change was not statistically significant (p = 0.151), reflecting variability among sampling sites and the strong buffering capacity of carbonate-rich soils. The reduction may be attributed to partial leaching of soluble carbonates during early rains in November or localized dissolution and redistribution processes. Nonetheless, the lack of statistical support indicates that carbonate dynamics are less sensitive to short-term climatic variability compared with other soil attributes.

The most striking seasonal differences were observed in parameters linked to salinity stress. Surface soil salinity decreased from 0.30 ± 0.13% in April to 0.15 ± 0.05% in November (p = 0.0067) (Table 3), representing a 50% reduction and a large effect size (Cohen's d = −1.11). Electrical conductivity (EC), a direct measure of soil salt concentration, exhibited a more pronounced decline, dropping by 65% from 704.1 ± 304.0 µS/cm in April to 246.0 ± 58.9 µS/cm in November ($p < 0.001$, d = −1.55). Similarly, total dissolved solids (TDSs) fell by 54% (1544.8 ± 681.8 mg/kg in April to 707.7 ± 168.5 mg/kg in November, p = 0.0031, d = −1.26) (Table 3).

These reductions are statistically robust and confirm the leaching effect of early seasonal rainfall [65], which flushes soluble salts downward through the soil profile. In semi-arid rangelands, salt accumulation during dry months can create osmotic stress, inhibiting plant water uptake. The statistically significant decreases in salinity, EC, and TDS from April to November therefore represent critical seasonal improvements in soil quality that directly benefit vegetation establishment and microbial functioning.

Soil moisture showed a substantial seasonal increase, rising from 3.88 ± 1.41% in April to 9.42 ± 2.52% in November (Table 3). This 143% increase was statistically significant (p = 0.037), underscoring the effectiveness of November rainfall in replenishing water reserves at the onset of the rainy season. Soil moisture is a key determinant of plant growth and rangeland productivity, and the observed increase provides quantitative evidence that seasonal rains substantially improve water availability for vegetation.

Organic matter content also increased markedly, from 7.11 ± 1.68% in April to 15.26 ± 1.72% in November (a 114% increase) (Table 3), which enhances soil structure and improves water retention capacity [66]. Despite the significant difference, statistical testing did not reveal significance (p = 0.78), suggesting high variability among sampling points. Nevertheless, the ecological implications are clear: the doubling of organic matter is consistent with the seasonal deposition of livestock manure, the decomposition of plant residues after the growing season, and reduced organic matter uptake by plants as growth slows in November. Although the change is not statistically significant, the magnitude of the increase supports the conclusion that organic matter dynamics are strongly influenced by seasonal grazing and rainfall.

Nutrient measurements revealed important seasonal patterns, although statistical tests could not be applied due to limited replication (n < 3). Despite this limitation, the magnitude of the observed changes provides valuable ecological insights. The average concentrations of NO_3^- declined by ~27%, from 35.3 mg/kg in April to 25.9 mg/kg in November (Table 4). The reduction is likely due to leaching and microbial denitrification [66] under wetter November conditions. SO_4^{2-} concentrations dropped sharply by ~72% (116.8 mg/kg in April to 32.7 mg/kg in November) (Table 4), consistent with leaching by rainfall. PO_4^{3-} levels more than doubled, increasing by 126% from 0.58 mg/kg in April to 1.30 mg/kg in November (Table 4). This increase may result from the decomposition of plant residues and reduced uptake by plants at the end of the growing season. Cl^- and F^- ions declined drastically, by −82% and −86%, respectively, again consistent with strong leaching processes (Table 4). And NO_2^- concentrations rose more than eightfold, from 0.41 mg/kg in April to 3.70 mg/kg in November (Table 4). This unusual increase may reflect the formation of anaerobic microsites in wetter soils, leading to incomplete denitrification. Although not statistically tested, these nutrient shifts provide a coherent picture of rainfall-driven flushing of mobile ions and nutrient redistribution within the soil profile.

Table 4. Statistics of soil samples parameters (April and November 2021).

Parameter	n (Pairs)	April Mean ± SD	November Mean ± SD	% Change	Statistical Test
Nitrate (mg/kg)	2	80.72 ± 0.00	58.48 ± 55.58	−27.5%	Not tested (n < 3)
Sulfate (mg/kg)	2	116.75 ± 0.00	32.67 ± 10.13	−72.0%	Not tested (n < 3)
Phosphate (mg/kg)	2	0.58 ± 0.00	1.30 ± 0.90	125.90%	Not tested (n < 3)
Chloride (mg/kg)	2	147.69 ± 0.00	26.05 ± 13.57	−82.4%	Not tested (n < 3)
Fluoride (mg/kg)	2	3.38 ± 0.00	0.48 ± 0.10	−85.7%	Not tested (n < 3)
Nitrite (mg/kg)	2	0.41 ± 0.00	3.70 ± 0.99	813.10%	Not tested (n < 3)

However, the subsurface samples revealed patterns that were distinct from those in the surface soils. Salinity levels remained constant at 0.1% across both sampling dates, indicating that salts leached from the surface were not yet accumulating strongly in deeper layers. TDS values declined moderately (664.5 mg/kg in April to 512.6 mg/kg in November), while pH dropped slightly from 8.0 to 7.6 (Table 5). Moisture content remained stable (6.6–6.9%) (Table 5), reflecting gradual infiltration of rainfall into deeper horizons. Organic matter in subsurface soils showed little change, remaining low at 7.4% in April and 6.7% in November (Table 5).

Table 5. Average values of sub-surface soil parameters for samples collected in April and November 2021.

Sampling Campaign	pH	TDS mg/Kg	Sal %	Moisture Content %	Organic Matter %	$CaCO_3$%	NO_3^- mg/Kg	PO_4^{3-} mg/Kg	SO_4^{2-} mg/Kg
April 5–21	8	664.5	0.1	6.6	7.4	27	48.3	0.4	114.4
Nov 29–21	7.6	512.6	0.1	6.9	6.7	19.3	32.7	1.1	35.1

In contrast, nitrate concentrations were substantially higher in subsurface soils compared with surface soils, reaching 48.3 mg/kg in April and 32.7 mg/kg in November (Table 5). This suggests a downward movement of nitrate from the surface to the subsoil layers during rainfall events. Phosphate concentrations also increased in November (from 0.4 to 1.1 mg/kg), consistent with the surface patterns. The results showed that subsurface soils appeared more buffered against seasonal changes, but the downward movement of nitrate and phosphate indicates active leaching and nutrient redistribution within the soil profile.

3.2. Land Use of Khanasri

The land use map of Al-Khanasri reserve highlights the spatial distribution of different land use types (Figure 4). The reserve area spans 300 hectares of natural rangelands. Cultivated areas (mostly barley) are estimated at 47 ha and are concentrated in the northeastern section. A protected military site, covering 12 hectares, is situated in the northern part of the reserve. Additionally, a small built-up area of 8 ha is located in the northwestern part, representing the research campus of Jordan's National Agricultural Research Center (NARC). This land-use distribution reflects a mixed-use landscape in which conservation, agricultural activities, and limited development coexist.

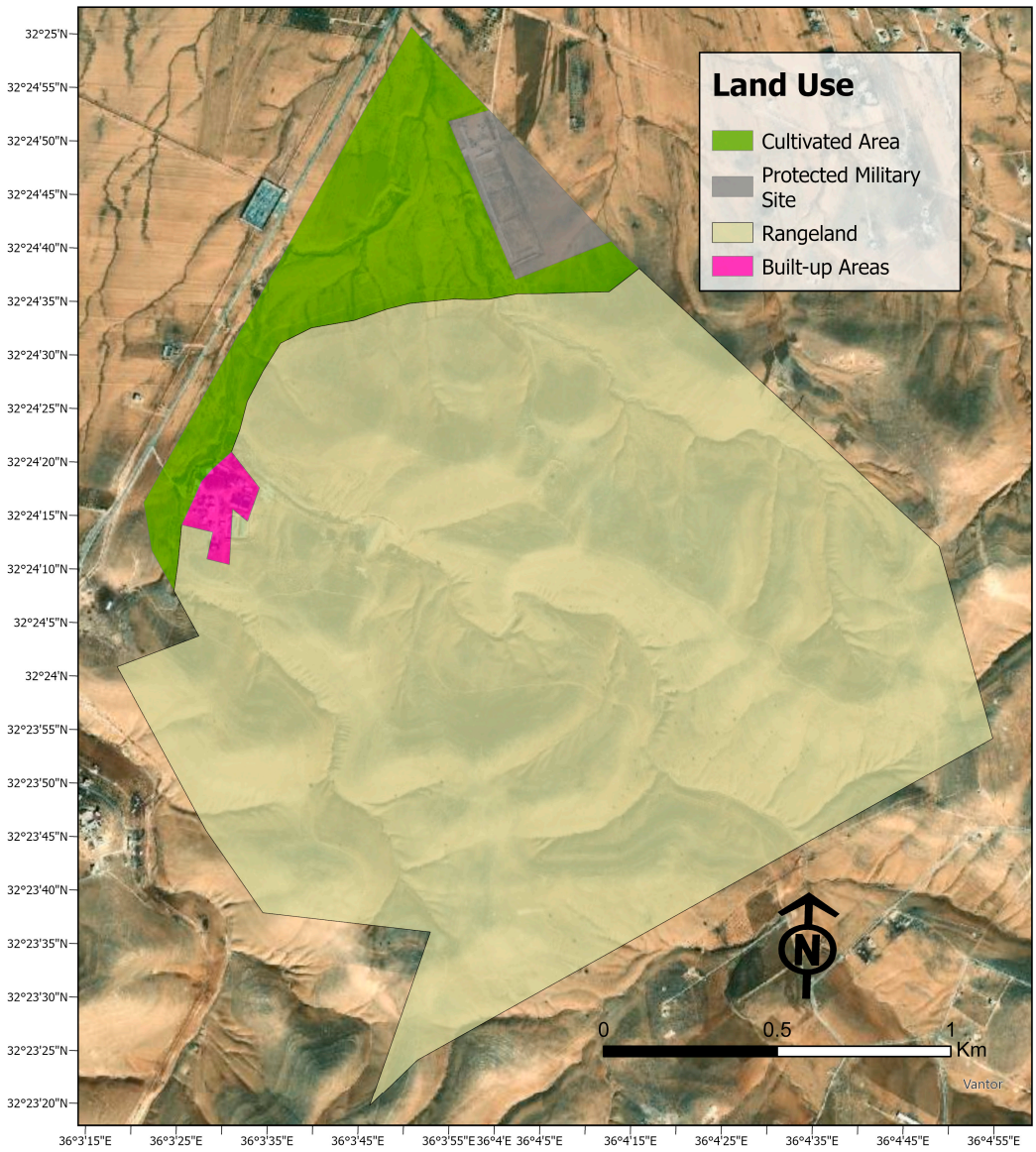


Figure 4. The land use map of Al-Khanasri reserve showing the spatial distribution of different land use types within the reserve.

3.3. Available Forage Biomass

The spatial distribution of above-ground vegetation biomass sampling locations within the Al-Khanasri range reserve illustrates a well-planned sampling strategy across diverse reserve areas. The five sampling locations are spatially dispersed to capture variability in vegetation production across different terrains and aspects. Locations 1 and 2 are situated in the reserve's northeastern and southern locations, respectively, characterized by higher vegetation density and specific ecological interest. Location 3 is positioned in the southern part, while locations 4 and 5 are in the western and northern regions, respectively, ensuring comprehensive spatial coverage. The productivity estimates for the five sampling locations, measured in kilograms per hectare per year, showed significant spatial variability in forage production (Table 6). Net productivity (available forage) varied substantially across locations, with the highest yields recorded in the north and the lowest in the southern site. Overall, the reserve's average yield suggests moderate productivity.

Table 6. The available forage across the 5 locations in Al-Khanasri.

Location #	Available Forage (kg/ha/year)
1	240
2	321
3	111
4	340
5	964

3.4. Vegetation Density (2016–2021)

NDVI time-series analysis showed clear interannual and seasonal fluctuations in vegetation density. Lower values were observed in 2016 and 2018, while higher cover was recorded in 2019 and 2021, reflecting the variability in rainfall across the years (Figure 5). Peak vegetation greenness consistently occurred in mid-March, coinciding with the growth season. Table 7 presents the relative average vegetation coverage based on NDVI classes, which were selected according to literature on arid and semi-arid regions [67,68].

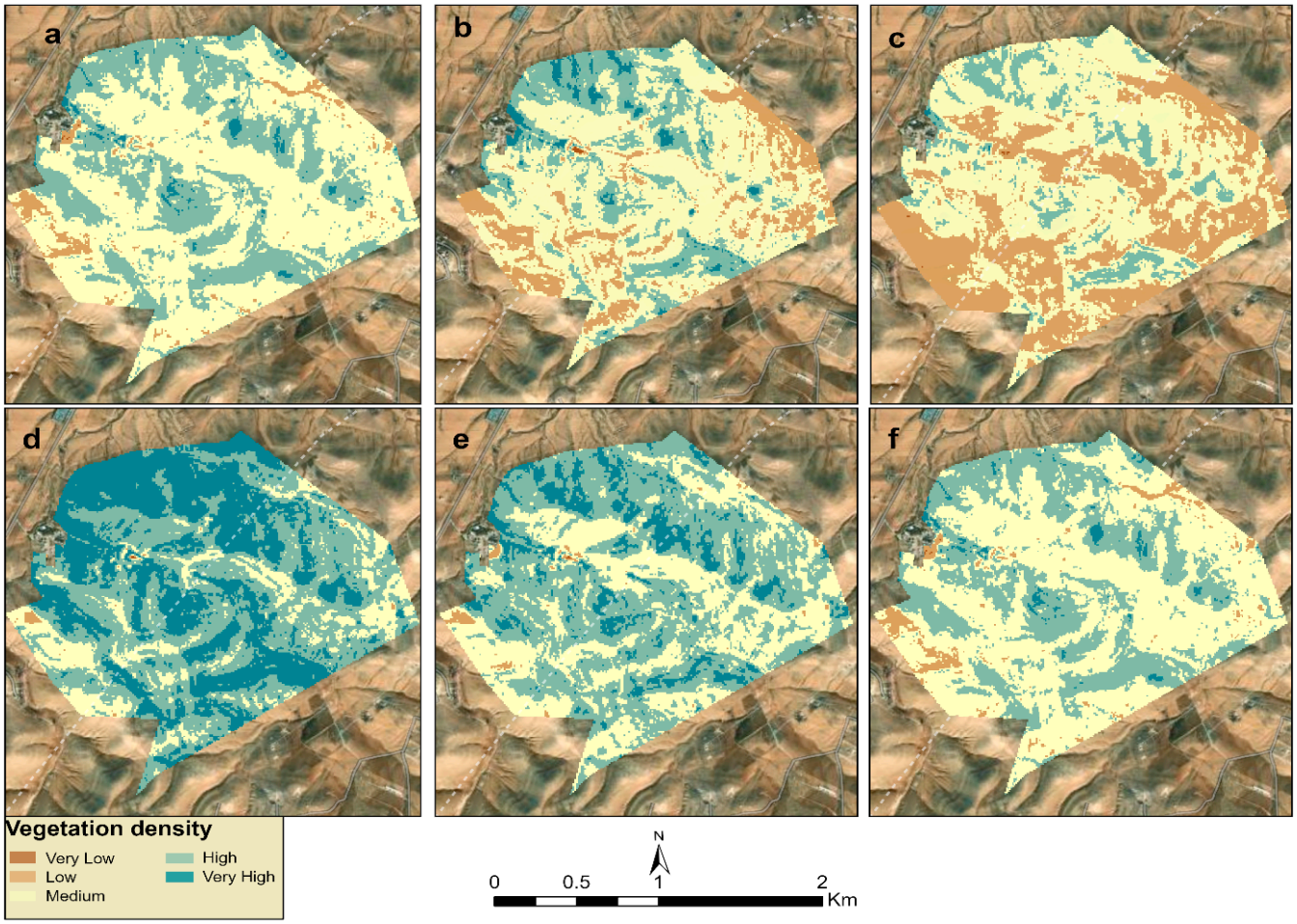


Figure 5. Vegetation biomass coverage derived from NDVI time-series for the Al-Khanasri reserve for the years: (**a**) 2016, (**b**) 2017, (**c**) 2018, (**d**) 2019, (**e**) 2020, and (**f**) 2021.

Table 7. Vegetation cover in Al-Khanasri reserve during the monitoring period.

		Relative Coverage (%)					
NDVI Range	**Average NDVI**	**2016**	**2017**	**2018**	**2019**	**2020**	**2021**
<0.1	Very low	<1	<1	<1	<1	<1	<1
0.1–0.2	Low	27.5	15	34	3	15.2	3.3
0.2–0.3	Medium	59.5	58	57	11.8	51.6	58.7
0.3–0.4	High	12.6	23	8	60.2	22.0	37
>0.4	Very high	<1	3	<1	25	11.0	<1

3.5. Plant Biodiversity of Al-Khanasri

The collected plant dataset provided a comprehensive inventory of 72 species found in the reserve, classified by their family, species, chorotype (geographical distribution), life form, and pastoral value (Table 8). The reserve supports a diverse flora, dominated by Asteraceae, Gramineae, and Fabaceae, with over 60% of species having good to excellent pastoral value, despite the presence of many species of low value. Regarding pastoral value, seven species (9.7%) were classified as excellent, 10 species (13.9%) as very good, and 28 species (38.9%) as good, while 27 species (37.5%) were weak in grazing value. Although weak-value species dominate numerically, they play an ecological role in stabilizing soils and sustaining biodiversity. The relatively high proportion of good to excellent forage plants (approximately 62.5%) underscores the reserve's potential to support livestock if managed sustainably. This balance between ecological protection and forage provision demonstrates the importance of conserving the reserve as a rangeland resource in arid and semi-arid regions.

Table 8. Dominant plant species found in the reserve, along with their pastoral values.

Plant Family	**Plant Species**	**Chorotype**	**Life Form**	**Pastoral Value**
Amaryllidaceae	*Ixiolirion tataricum*	Irano-Turanian	geophyte	Good
Apiaceae	*Foeniculum vulgare*	Med-Irano-Turanian	hemicryptophyte	Good
Apiaceae	*Pimpinella cretica*	Mediterranean	Annual	Good
Apiaceae	*Torilis leptophylla*	Med-Irano-Turanian	Annual	Good
Asteraceae	*Achillea fragrantissima*	Irano-Turanian-Saharo-Arabian	perennial shrub/hemicryptophyte	Weak
Asteraceae	*Anthemis palestina*	Mediterranean	Annual/chamaephyte	Weak
Asteraceae	*Artemisia sieberi*	Irano-Turanian	perennial shrub	Very good
Asteraceae	*Carduus australis*	Carduus australis	Annual	Weak
Asteraceae	*Carthamus tenuis*	Mediterranean	Annual	Weak
Asteraceae	*Centaurea iberica*	Med-Irano-Turanian	perennial herb	Weak
Asteraceae	*Crepis aspera*	Mediterranean	Annual	Good
Asteraceae	*Crepis sancta*	Med-Saharo-Arabian	Annual	Good
Asteraceae	*Filago contracta*	Irano-Turanian	Annual	Good
Asteraceae	*Filago desertorum*	Irano-Turanian-Saharo-Arabian	Annual	Good
Asteraceae	*Gymnarrhena micrantha*	Saharo-Arabian	Annual	Very good

Table 8. *Cont.*

Plant Family	Plant Species	Chorotype	Life Form	Pastoral Value
Asteraceae	*Lactuca serriola*	Euro-Siberian-Med-Irano-Turanian	Annual herb	Very good
Asteraceae	*Lactuca orientalis*	chamaephyte	perennial herb	Very good
Asteraceae	*Scorzonera papposa*	Irano-Turanian	perennial/hemicryptophyte	Excellent
caryophyllaceae	*Gypsophila capillaris*	Irano-Turanian	chamaephyte	Weak
caryophyllaceae	*Minuartia picta*	Irano-Turanian	Annual	Weak
caryophyllaceae	*Paronychia argentea*	Mediterranean	hemicryptophyte	Weak
caryophyllaceae	*Silene arabica*	Saharo-Arabian	Annual	Good
caryophyllaceae	*Silene colorata*	Mediterranean	Annual	Good
Chenopodiaceae	*Anabasis articulata*	Saharo-Arabian	chamaephyte	Good
Chenopodiaceae	*Noaea mucronata*	Irano-Turanian	chamaephyte	Weak
Chenopodiaceae	*Salsola vermiculata*	Irano-Turanian-Saharo-Arabian	chamaephyte	Excellent
Chenopodiaceae	*Atriplex halimus*	Med-Saharo-Arabian	phanerophyte shrub	Good
Crassulaceae	*Sedum rubens*	Med-Euro-Siberian	Annual	Weak
Cruciferae	*Neotorularia torulosa*	Irano-Turanian	Annual	Very good
Ephedraceae	*Ephedra alata*	Saharo-Arabian	chamaephyte	Good
Fabaceae	*Astragalus callichrous*	Saharo-Arabian	Annual	Weak
Fabaceae	*Astragalus asterias*	Med-Saharo-Arabian	Annual	Weak
Fabaceae	*Hippocrepis unisiliquosa*	Mediterranean	Annual	Good
Fabaceae	*Medicago rotata*	Mediterranean	Annual	Good
Fabaceae	*Melilotus officinalis*	Mediterranean	annual	Good
Fabaceae	*Onobrychis caput-galli*	Mediterranean	Annual	Excellent
Fabaceae	*Retama raetam*	Saharo-Arabian	phanerophyte shrub	Weak
Fabaceae	*Trigonella caelesyriaca*	Mediterranean	Annual	Good
Fabaceae	*Trigonella stellata*	Saharo-Arabian	Annual	Good
Fabaceae	*Vicia peregrina*	Med-Irano-Turanian	Annual	Excellent
Fumariaceae	*Fumaria densiflora*	Mediterranean	Annual	Very good
Geraniaceae	*Erodium ciconium*	Med-Irano-Turanian	Annual	Excellent
Gramineae	*Aegilops biuncialis*	Mediterranean	Annual	Very good
Gramineae	*Avena sterilis*	Med-Irano-Turanian	Annual	Good
Gramineae	*Bromus tectorum*	Med-Irano-Turanian-Saharo-Arabian	Annual	Good
Gramineae	*Dactylis glomerata*	Euro-Siberian-Med-Irano-Turanian	hemicryptophyte	Excellent
Gramineae	*Hordeum bulbosum*	Med-Irano-Turanian	hemicryptophyte	Good
Gramineae	*Hordeum glaucum*	Med-Irano-Turanian	Annual	Good
Gramineae	*Hordeum spontaneum*	Med- Irano-Turanian	Annual	Good
Gramineae	*Lagurus ovatus*	Mediterranean	Annual	Good
Gramineae	*Phalaris minor*	Med-Irano-Turanian	Annual	Good
Gramineae	*Poa eigii*	Irano-Turanian	hemicryptophyte	Good
Gramineae	*Rostraria cristata*	Med-Irano-Turanian	Annual	Excellent
Gramineae	*Schismus arabicus*	Irano-Turanian-Saharo-Arabian	Annual	Good
Gramineae	*Stipa capensis*	Irano-Turanian-Saharo-Arabian	Annual	Excellent
Iridaceae	*Moraea sisyrinchium*	Med-Irano-Turanian	geophyte	Weak
Labiatae	*Ajuga iva*	Mediterranean	chamaephyte	Very good

Table 8. *Cont.*

Plant Family	Plant Species	Chorotype	Life Form	Pastoral Value
Labiatae	*Salvia dominica*	Mediterranean	chamaephyte	Weak
Liliaceae	*Allium ampeloprasum*	Med-Irano-Turanian	geophyte	Weak
Malvaceae	*Malva nicaeensis*	Med-Irano-Turanian	Annual	Very good
Papaveraceae	*Papaver hybridum*	Med-Irano-Turanian	Annual	Very good

3.6. GIS-Based MCDA Rangeland Grazing Suitability

3.6.1. Factor-Wise Reserve Suitability

The assessment of soil moisture suitability within the rangelands indicates that only 1.3% of the total area is classified as marginally suitable for grazing (Figure 6). A substantial 98.7% is deemed unsuitable due to insufficient soil moisture availability. Despite these constraints, the analysis of organic matter content reveals that the rangelands exhibited high suitability for soil fertility, suggesting that while moisture availability is a limiting factor for grazing, the organic composition of the soil is not a significant constraint. The evaluation of vegetation density attributes highlighted a limited extent of highly suitable grazing areas within the rangelands. Specifically, less than 1% of the area exhibits vegetation density levels that are favorable for optimal grazing. Approximately 15% of the rangeland area is classified as moderately suitable, and 84% falls within the marginally suitable category (Figure 6). The slope suitability result indicates that 13% of the range terrain is highly suitable for grazing, while 11% is moderately suitable. The findings suggest that most range reserve areas are marginally suitable for grazing, implying that terrain inclination may challenge livestock movement and forage accessibility.

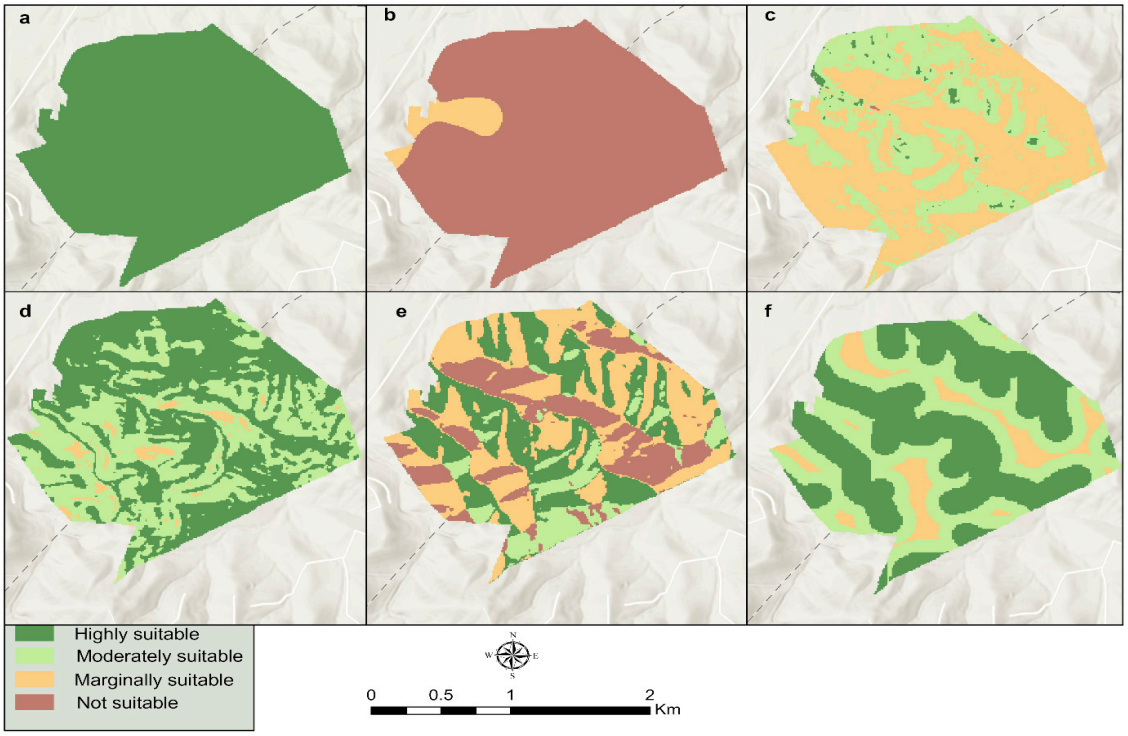


Figure 6. Factor suitability map for livestock grazing: (**a**) soil organic matter, (**b**) soil moisture content, (**c**) average NDVI, (**d**) slope, (**e**) aspect, and (**f**) water accessibility.

The aspect suitability analysis indicated that slopes facing north and northwest, which provide the most favorable conditions for grazing, constituted 29.7% of the rangeland area. Moderately suitable aspects accounted for 11.5%, while 38.3% were marginally suitable

for grazing. 20.5% of the rangeland slopes facing south and southwest are considered unsuitable for grazing due to their exposure to higher solar radiation and drier conditions. Suitability analysis of water accessibility indicated that 49% of the rangeland area was highly suitable for livestock grazing, while 40% was moderately suitable. Only 11% of the rangeland was marginally suitable for grazing. These results suggest that most grazing areas are close to major wadis that traverse the relatively small reserve, allowing for short travel distances and ease of movement for sheep and goats. Consequently, water availability is not a significant constraint for livestock grazing within the study area, particularly given the presence of a water-harvesting project on the major wadi of the reserve.

3.6.2. Final Grazing Suitability of the Al-Khanasri Reserve for Livestock

The final suitability map of the range reserve for grazing shows that 13.8% of the Al-Khanasri rangelands were classified as highly suitable, offering optimal conditions for grazing (Figure 7). Additionally, 24.4% of the rangelands were moderately suitable, suggesting that while grazing is feasible, certain environmental constraints may limit productivity. A significant portion, 39% of the rangeland area, fell within the marginally suitable category, where grazing is possible but subject to limitations such as low vegetation cover, poor soil moisture, or topographic constraints. Furthermore, 22.8% of the rangeland is considered unsuitable for livestock production, highlighting areas where environmental conditions do not support sustainable grazing practices.

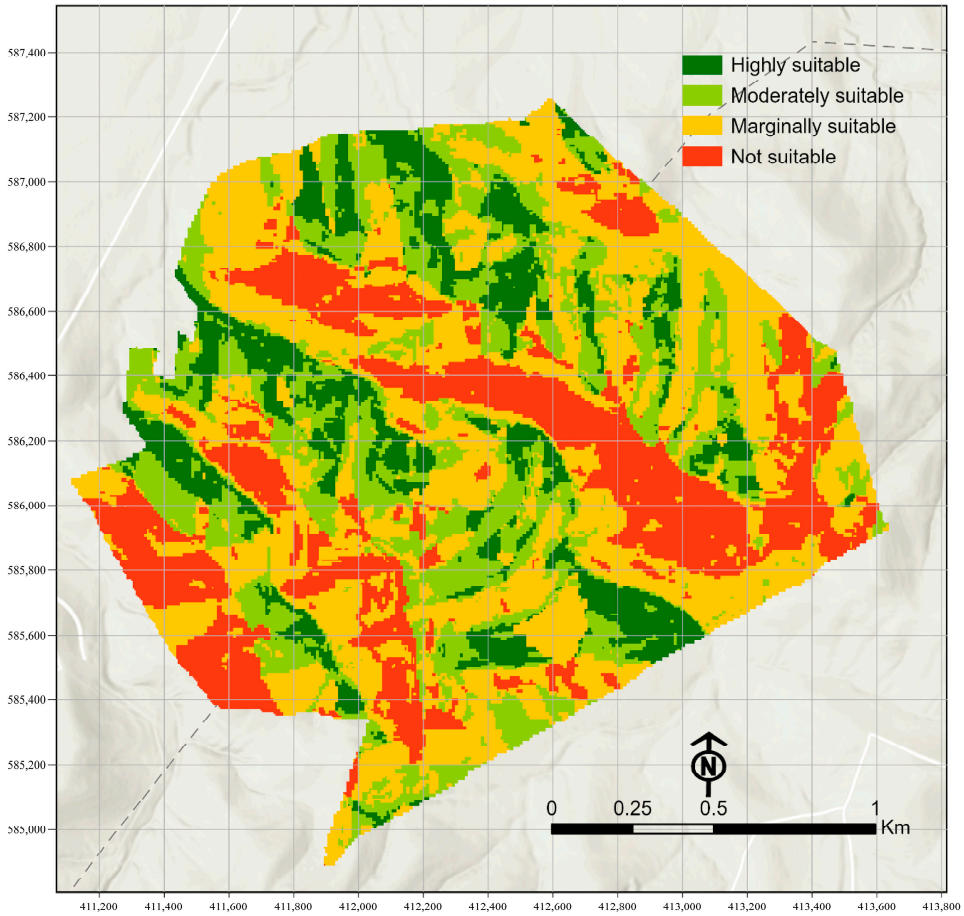


Figure 7. Range suitability map for livestock grazing.

4. Discussion

This study provides new insights into the ecological dynamics and grazing suitability of the Al-Khanasri reserve by integrating soil and vegetation measurements with multi-season remote sensing data. The results highlight seasonal variability in soil attributes, forage productivity, and vegetation cover, while the suitability framework identifies both highly suitable areas for grazing and zones requiring careful management. These findings underscore the importance of developing evidence-based strategies that balance livestock production and ecosystem resilience in semi-arid environments. Recent studies in Jordan support and extend these results. Haddad et al. [6] demonstrated that combining protection with hydrological restoration improves soil water retention and vegetation recovery, while Strohmeier et al. [21] found that micro-water harvesting with native shrub planting enhances rangeland resilience. The Healthy Ecosystems for Rangeland Development (HERD) initiative further underscores the role of sustainable pastoral practices and participatory monitoring [69]. Our study advances this body of work by explicitly classifying rangeland suitability for sheep and goats (S1–N1) and integrating field data with remote sensing to provide a refined, spatially explicit tool for guiding grazing management and restoration in Jordan's drylands.

4.1. Impacts of Managed Grazing on Seasonal Variation in Soil Attributes

Rainfall emerges as the dominant control on soil dynamics in the Al-Khanasri Reserve. Across seasons, the soil pH remained stable, consistent with carbonate buffering, which maintains slightly alkaline conditions conducive to micronutrient availability [66]. Carbonate content likewise showed no meaningful change, underscoring the inherent stability of $CaCO_3$-rich substrates. In contrast, salinity-related attributes declined sharply from April to November, with salinity decreasing by ~50%, electrical conductivity (EC) by ~65%, and total dissolved solids (TDSs) by ~54%, each exhibiting a large effect size. These coherent, statistically significant shifts indicate efficient leaching of salts with the onset of early seasonal rains, thereby alleviating osmotic stress and improving the edaphic environment for vegetation.

Soil moisture exhibited a statistically significant increase, more than doubling between April and November, confirming the role of seasonal precipitation in replenishing soil water reserves essential for rangeland productivity. Although the rise in organic matter (OM) was not statistically significant ($p = 0.78$; Table 3), the observed doubling is ecologically meaningful. Heterogeneous manure inputs and plant-residue distribution likely elevate variance and reduce statistical power; however, the direction and magnitude of change suggest that November soils are consistently enriched in organic inputs that enhance aggregation, water retention, and nutrient cycling.

Nutrient behavior further corroborates rainfall-driven processes. Nitrate concentrations declined by ~27% from April to November, consistent with leaching, reduced nitrification under cooler conditions, and enhanced denitrification in wetter soils [70]. Higher subsurface nitrate levels than surface nitrate support downward movement. Sulfate, chloride, and fluoride decreased markedly (−72% to −86%; Table 4), matching the leaching signal. In contrast, phosphate more than doubled, plausibly reflecting residue decomposition and reduced plant uptake toward the end of the growing season, with positive implications for early-season growth in subsequent years. Nitrite levels increased, suggesting the presence of transient anaerobic microsites within the wetter November soils. While small sample sizes limited formal testing for some ions, the patterns align with established soil biogeochemical pathways and are ecologically consistent.

These coupled statistical and ecological signals have clear management implications. In April, soils are drier, more saline, and relatively nutrient-depleted due to high evapora-

tive demand and active plant uptake; heavy grazing at this time risks compounding stress, accelerating surface salt accumulation, and suppressing forage recovery. By November, soils are measurably moister, substantially less saline, and enriched in organic inputs, offering a window more conducive to vegetation regeneration. Strategically timing grazing to the wetter months supports nutrient cycling while minimizing pressure on recovering plant communities. Although the increase in OM lacked statistical significance, the directional change, together with evidence of manure deposition, highlights the contribution of managed grazing to soil fertility and structure [62].

The findings suggest that seasonal rainfall serves as a natural reset mechanism in this semi-arid rangeland, mitigating salinity stress, replenishing moisture, and regulating nutrient availability. Interpreting the dataset through both statistical significance (salinity, EC, TDS, moisture) and ecological significance (OM and selected nutrients) provides a balanced basis for decision-making. Adaptive grazing regimes that restrict stocking during dry months and emphasize controlled use during wetter periods are likely to conserve soil organic matter, sustain vegetation vigor, and enhance the resilience of the Al-Khanasri system.

4.2. Assessment of Vegetation Biomass and Plant Diversity

The productivity results indicate a notable spatial variability in forage yield across the reserve. Location #5 demonstrates the highest productivity at 964 kg/ha/year, likely due to favorable biophysical conditions such as soil fertility, moisture availability, or moderated grazing impact. It was reported that a dry yield of a protected site in the Al-Khanasri area was 923.16 kg/ha [23]. Location 3 shows the lowest productivity at 111 kg/ha/year, suggesting constraints related to overgrazing, shallow soil depth, or exposure to environmental stressors. The overall average dry yield of the reserve was 395 kg/ha/year, aligning with other studies in similar environments [11], which estimated that dry forage production levels range from 200 to 800 kg/ha/year in low-rainfall areas. Strohmeier et al. [21] reported biomass values from 350 to 900 kg/ha/year in rehabilitated micro-catchments. Therefore, our measured average yield of 395 kg/ha/year can be considered moderate and generally within the expected range for managed steppe rangelands.

The influence of managed grazing on vegetation density and forage productivity becomes evident through time-series NDVI analysis derived from Sentinel-2 data from 2016 to 2021. The NDVI trends indicate fluctuating vegetation cover, with relatively lower values in 2016 and 2018, which may correspond to low rainfall rates or inadequate grazing regulation. The cumulative rainfall rate in the 2015–2016 rainy season, as calculated from the climate station in the area, was 100 mm. A marked improvement in NDVI values was observed in 2017, 2019, and 2020—especially in 2019, which exhibited the highest vegetation density, likely due to improved rainfall and active conservation or grazing exclusion measures. The proportion of the area classified as having high vegetation density (NDVI 0.3–0.4) increased dramatically from 12.6% in 2016 to 60.2% in 2019, indicating significant ecological recovery. Likewise, very high vegetation density (NDVI > 0.4), although generally limited, showed peaks in 2017 (3%), 2019 (25%), and 2020 (11%). This can be attributed to the increase in rainfall rate, as the cumulative rainfall during the 2018–2019 rainy season reached 230 mm. The marked increase in vegetation density observed in 2019 was not limited to our study area; similar trends were noted throughout the northern Badia. This phenomenon could be attributed to COVID-19 lockdown measures, which effectively acted as a region-wide grazing conservation strategy [34].

The analysis of pastoral values of the identified plant communities in the range reserve revealed that 22% of the reserve's plant species were classified as having excellent to very good forage potential, primarily from the *Asteraceae*, *Gramineae* (*Poaceae*), and

Fabaceae families. Additionally, 39% were categorized as good forage species, 23% had low forage value, and 16% were non-palatable or potentially toxic to livestock. The practice of managed grazing in such ecosystems has yielded multifaceted impacts on biodiversity. In Mediterranean rangelands, moderate and rotational grazing regimes help maintain species richness, prevent the dominance of unpalatable or invasive species, and support ecosystem resilience [13,71]. Studies on Jordanian reserves, including the Badia region, have demonstrated that community-based grazing management enhances vegetation cover and supports the restoration of key species [12,13]. The reserve supports a diverse range of Mediterranean, Irano-Turanian, and Saharo-Arabian plant species, with 22% classified as excellent or very good for grazing. However, 16% of species are non-pastoral or toxic, posing risks to livestock health and necessitating careful management of grazing. The dominance of shrubland vegetation and limited tree cover further restricts the availability of high-quality forage, highlighting the need for supplementary feeding strategies and seasonal grazing adjustments [72].

4.3. Determinants of Reserve Grazing Suitability

Topographic features strongly influence grazing suitability in dryland rangelands, affecting forage productivity and livestock movement [28,38]. In the Al-Khanasri Reserve, only 13% of the terrain is highly suitable for grazing, while another 11% is moderately suitable. By contrast, much of the reserve exhibits steep inclines or south- and southwest-facing aspects, which receive higher solar radiation and retain less soil moisture, making them marginal or unsuitable for sustained grazing [13,21]. Water availability further modulates grazing distribution [8,11]. Nearly half of the reserve area (49% relative coverage) is located near wadis and other water sources, making these areas highly suitable for livestock. An additional 40% is moderately suitable for grazing based on water access, which helps mitigate the arid climate's inherent constraints by reducing stress on livestock and preventing overuse of any single watering point. Despite these topographic and hydrological limitations, Al-Khanasri's moderate grazing suitability can be enhanced through strategic measures. Erosion control, rotational grazing, and restoration of high-quality forage stands can bolster ecological resilience and sustain livestock productivity. Such integrated land management practices, often applied in similar Jordanian and Mediterranean rangelands, have consistently demonstrated long-term benefits for both herders and the broader ecosystem [21].

5. Conclusions and Limitations

This study presented a comprehensive and integrated approach to evaluating the Suitability of the Al-Khanasri Reserve for livestock grazing, utilizing remote sensing, Geographic Information System (GIS)-based Multi-Criteria Decision Analysis (MCDA), and field-based measurements. The analysis underscored the critical importance of spatially explicit assessments in the sustainable management of semi-arid rangelands. Key biophysical factors—including soil characteristics, vegetation cover, topographic features, and water accessibility—were analyzed collectively to determine their influence on grazing potential. While the reserve possesses certain favorable attributes, particularly regarding water accessibility and organic matter content, its overall suitability for grazing is limited by soil moisture availability, sparse vegetation density, and steep terrain. The study generates a replicable model for rangeland monitoring and targeted grazing management. It effectively identified optimal grazing zones and areas requiring ecological restoration or protection. Integrating satellite-derived vegetation indices with ground-based biomass assessments enables temporal monitoring of vegetation dynamics and contributes to adaptive management strategies. To enhance livestock productivity while mitigating degradation

risks, the study advocates for sustainable grazing practices, including rotational grazing, supplementary feeding during dry periods, and the conservation of high-value forage areas. While this study employed detailed soil, vegetation, and remote sensing data to establish a robust framework, future monitoring may not require replicating the same level of sampling complexity. A simplified framework that focuses on key variables —such as rainfall, soil depth, slope, and vegetation indices —can provide reliable insights for long-term monitoring and management. This approach ensures that the methodology remains both scientifically rigorous and practically applicable for routine rangeland assessments.

Despite its significant contributions, the study has limitations. Upscaling in situ soil and vegetation data to satellite-derived maps may introduce spatial uncertainty into predictive models. Additionally, the lack of long-term grazing pressure data restricts the ability to fully assess the cumulative impacts of livestock activity on rangeland health. Future research should incorporate high-resolution remote sensing technologies, machine learning approaches for land classification, and participatory methods involving local pastoral communities. Such advancements will be essential for refining suitability assessments and supporting the long-term sustainability and resilience of grazing systems in arid and semi-arid environments.

Author Contributions: R.N.J.: Led the research project, designed the study, conducted field sampling, performed data analysis, and drafted the manuscript. Z.M.: Conducted fieldwork, contributed to data analysis, and revised the manuscript. N.O.: Assisted with fieldwork, facilitated communication with local communities, and supported manuscript writing, particularly sections on productivity and Biodiversity. A.A.-T.: Revised the manuscript and contributed to writing sections related to soil analysis and results. All authors have read and agreed to the published version of the manuscript.

Funding: This research was funded by the Scientific Research and Innovation Support Fund at the Ministry of Higher Education and Scientific Research in Jordan, grant number WE/1/15/2018.

Data Availability Statement: The original contributions presented in the study are included in the article, further inquiries can be directed to the corresponding author.

Acknowledgments: The authors sincerely thank Mustafa Al-Shdeifat, Director of Al-Khanasri Reserve, Ahed Obeidat, former Director of the Northwestern Badia Agriculture Directorate, the National Agricultural Research Center (NARC), and those who assisted in collecting soil and plant samples, provided valuable support, facilitating research activities at the reserve and offering valuable livestock statistics for the study area.

Conflicts of Interest: The authors declare no conflicts of interest.

References

1. Lambin, E.F.; Ehrlich, D. Land-cover changes in Sub-Saharan Africa (1982–1991): Application of a change index based on remotely sensed surface temperature and vegetation indices at a continental scale. *Remote Sens. Environ.* **1997**, *61*, 181–200. [CrossRef]
2. Diouf, A.; Lambin, E. Monitoring land-cover changes in semi-arid regions: Remote sensing data and field observations in the Ferlo, Senegal. *J. Arid. Environ.* **2001**, *48*, 129–148. [CrossRef]
3. Lioubimtseva, E.; Cole, R.; Adams, J.; Kapustin, G. Impacts of climate and land-cover changes in arid lands of Central Asia. *J. Arid. Environ.* **2005**, *62*, 285–308. [CrossRef]
4. Rjili, H.; Muñoz-Ulecia, E.; Bernués, A.; Jaouad, M.; Martin-Collado, D. Evolution of pastoral livestock farming on arid rangelands in the last 15 years. *Animal* **2023**, *17*, 100748. [CrossRef]
5. Karatassiou, M.; Parissi, Z.M.; Panajiotidis, S.; Stergiou, A. Impact of grazing on diversity of semi-arid rangelands in Crete Island in the context of climatic change. *Plants* **2021**, *11*, 982. [CrossRef]
6. Haddad, M.; Strohmeier, S.M.; Nouwakpo, K.; Rimawi, O.; Weltz, M.; Sterk, G. Rangeland restoration in Jordan: Restoring vegetation cover by water harvesting measures. *Int. Soil. Water Conserv. Res.* **2022**, *10*, 610–622. [CrossRef]
7. Asner, G.P.; Elmore, A.J.; Olander, L.P.; Martin, R.E.; Harris, A.T. Grazing systems, ecosystem responses, and global change. *Annu. Rev. Environ. Resour.* **2004**, *29*, 261–299. [CrossRef]

8. Louhaichi, M.; Toshpulot, R.; Moyo, H.P.; Belgacem, A.O. Effect of slope aspect on vegetation characteristics in mountain rangelands of Tajikistan: Considerations for future ecological management and restoration. *Afr. J. Range Forage Sci.* **2021**, *39*, 320–328. [CrossRef]
9. Baloyi, T.M.; Maphanga, T.; Madonsela, B.S.; Grangxabe, X.S.; Malakane, K.C.; Munjonji, L. A review of community-based strategies for addressing bush encroachment in the semi-arid savannah rangelands of Southern Africa. *Conservation* **2025**, *5*, 15. [CrossRef]
10. Ibañez, J.; Valderrama, J.M.; Papanastasis, V.; Evangelou, C.; Puigdefabregas, J. A multidisciplinary model for assessing degradation in Mediterranean rangelands. *Land. Degrad. Dev.* **2014**, *25*, 468–482. [CrossRef]
11. Abu-Zanat, M.; Ruyle, G.; Abdel-Hamid, N. Increasing range production from fodder shrubs in low rainfall areas. *J. Arid. Environ.* **2004**, *59*, 205–216. [CrossRef]
12. Oweis, T.; Benli, B.; Bruggeman, A.; Farahani, H. (Eds.) *Characteristics of Benchmark Research Agroecosystems in WANA: Rainfed, Irrigated, and Marginal Drylands*; ICARDA: Aleppo, Syria, 2006; p. 98.
13. Al-Tabini, R.; Al-Khalidi, K.; Al-Shudiefat, M. Livestock, medicinal plants and rangeland viability in Jordan's Badia: Through the lens of traditional and local knowledge. *Pastoralism* **2012**, *2*, 4. [CrossRef]
14. Karadsheh, L.; Mazahreh, N.; Rawajfih, Z. Soil salinity changes in the Jordan Valley in relation to irrigation water. *Agric. Water Manag.* **2012**, *104*, 43–48. [CrossRef]
15. Food and Agriculture Organization (FAO). *Guidelines for the Preparation of the Country Reports for The State of the World's Biodiversity for Food and Agriculture*; FAO: Rome, Italy, 2013. Available online: https://openknowledge.fao.org/server/api/core/bitstreams/b29b1ccc-e00c-4b2c-8265-828a898d45ae/content (accessed on 15 May 2025).
16. Ministry of Agriculture, Directorate of Rangelands and Badia Development. *Updated Rangeland Strategy for Jordan 2013/2014*; Ministry of Agriculture: Amman, Jordan, 2013. Available online: https://faolex.fao.org/docs/pdf/jor165720.pdf (accessed on 18 September 2025).
17. Jawarneh, R.N.; Biradar, C.M. Decadal National Land Cover Database for Jordan at 30 m resolution. *Arab. J. Geosci.* **2017**, *10*, 483. [CrossRef]
18. Jawarneh, R.N.; Abulibdeh, A.; Hashem, N.; Awawdeh, M.; Al-Awadhi, T.; Abdullah, M.M.; El Kenawy, A.M. Assessing and predicting land cover dynamics for environmental sustainability in Jordan's arid ecosystems using CA-Markov model. *Remote Sens. Appl. Soc. Environ.* **2024**, *35*, 101262. [CrossRef]
19. Al-Taani, A.A. Comments on "Assessing rangeland cover conversion in Jordan after the Arab spring using a remote sensing approach" authored by Sawalhah et al. (2018). *J. Arid. Environ.* **2019**, *166*, 77–78. [CrossRef]
20. Myint, M.; Westerberg, V. *Jordan Case Study: An Economic Valuation of a Large-Scale Rangeland Restoration Project through the Hima System in Jordan*; Economics of Land Degradation Initiative (ELD): Bonn, Germany, 2015. Available online: https://repo.mel.cgiar.org/items/65d5487f-fae7-4c1b-81e6-d3097b23cf9c (accessed on 10 May 2025).
21. Strohmeier, S.; Fukai, S.; Haddad, M.; Al Nsour, M.; Mudabber, M.; Akimoto, K.; Yamamoto, S.; Evett, S.; Oweis, T. Rehabilitation of degraded rangelands in Jordan: The effects of mechanized micro-water harvesting on hill-slope scale soil water and vegetation dynamics. *J. Arid. Environ.* **2021**, *185*, 104338. [CrossRef]
22. Makhamreh, Z. Land degradation vulnerability assessment based on land use changes and FAO suitability analysis in Jordan. *Span. J. Soil. Sci.* **2019**, *9*, 3900. [CrossRef]
23. Al-Satari, Y.; Soub, H.; Oklah, M.; Amayreh, I. Assessment of effect of rangeland protection in Khanasri area of northern Badia region of Jordan. *Res. Crops* **2012**, *13*, 219–222.
24. Al-Okouri, A.; Al-Satari, Y.; Al-Tawarah, K.; Al-Khawaldeh, S.; Al-Jazazzi, S.M. The effect of rangeland protection on the native vegetation productivity at Shoubak in Jordan. *Int. J. Agric. Sci. Res.* **2014**, *4*, 107–112.
25. Flombaum, P.; Sala, O.E. A non-destructive and rapid method to estimate biomass and aboveground net primary production in arid environments. *J. Arid. Environ.* **2007**, *69*, 352–358. [CrossRef]
26. Monzingo, D.S.; Shipley, L.A.; Cook, R.C.; Cook, J.G. Factors influencing predictions of understory vegetation biomass from visual cover estimates. *Wildl. Soc. Bull.* **2022**, *46*, e1300. [CrossRef]
27. Salem, I.B.; Nazzal, Y.; Sharma, M.; Howari, F.M.; Kumaresan, P.R.; Karthi, A.; Al-Taani, A.A.; Maloukh, L.; Xavier, C. Mapping and monitoring of mangrove species in Eastern Lagoon National Park, Abu Dhabi, using Landsat 8 OLI data. *Arab. J. Geosci.* **2024**, *17*, 118. [CrossRef]
28. İleri, O.; Koç, A. Monitoring the available forage using Sentinel-2-derived NDVI data for sustainable rangeland management. *J. Arid. Environ.* **2022**, *200*, 104727. [CrossRef]
29. Bailey, D.; Al Tabini, R.; Horton, H.; Libbin, J.; Al-Khalidi, K.; Alqadi, A.; Al Oun, M.; Waldron, B. Potential for use of *Kochia prostrata* and perennial grasses for use in rangeland rehabilitation in Jordan. In Proceedings of the 17th International Farm Management Congress, Bloomington/Normal, IL, USA, 19–24 July 2009.
30. Al-Karablieh, E.; Jabarin, A. Different rangeland management systems to reduce livestock feeding costs in arid and semi-arid areas in Jordan. *Q. J. Int. Agric.* **2010**, *49*, 91–109.

31. Sawalhah, M.; AlShdifat, M.; Al-Kofahi, S.; Almasaeid, O. Enhancing semi-arid ecosystem resilience in Jordan using controlled grazing—A short- and long-term assessment. *J. Ecol. Eng.* **2024**, *25*, 29–42. [CrossRef]
32. Al-Karablieh, E. Effects of socioeconomic factors on rangeland institutional options in the semi-arid regions of Jordan. *Jordan J. Agric. Sci.* **2010**, *6*, 437–451.
33. Sawalhah, M.N.; Al-Kofahi, S.D.; Othman, Y.A.; Cibils, A.F. Assessing rangeland cover conversion in Jordan after the Arab spring using a remote sensing approach. *J. Arid. Environ.* **2018**, *157*, 97–102. [CrossRef]
34. Sawalhah, M.; Othman, Y.; Abu Yahya, A.; Al-Kofahi, S.; Al-Lataifeh, F.; Cibils, A. Evaluating the influence of COVID-19 pandemic lockdown on Jordan Badia rangelands. *Arid. Land. Res. Manag.* **2021**, *35*, 483–495. [CrossRef]
35. Al-Bakri, J.; Taylor, J. Application of NOAA AVHRR for monitoring vegetation conditions and biomass in Jordan. *J. Arid. Environ.* **2003**, *54*, 579–593. [CrossRef]
36. Alizadeh, E.; Arzani, H.; Azarnivand, H.; Mohajeri, A.; Kaboli, S.H. Range suitability classification for goats using GIS: Case study of Ghareaghach Watershed-Semirom. *Iran. J. Range Desert Res.* **2012**, *18*, 353–364.
37. Omidvar, E.; Mohtashamnia, S. Rangeland suitability for sheep grazing in semi-steppic rangelands of Tornas Eghlid, Fars Province, using GIS. *Renew. Nat. Resour. Res.* **2015**, *6*, 65–78.
38. Farazmand, A.; Arzani, H.; Javidi, S.; Sanadgol, A. Determining the factors affecting rangeland suitability for livestock and wildlife grazing. *Iran. J. Range Desert Res.* **2019**, *26*, 101–115. [CrossRef]
39. Balew, A.; Legese, B.; Kunbushu, D.; Nega, W.; Alebel, W.; Kerbesh, A.; Rahman, M.M. Identification of suitable land for livestock production using GIS-based multicriteria decision analysis and remote sensing in the Bale Lowlands, Ethiopia. *Int. J. Ecol.* **2022**, *2022*, 9585552. [CrossRef]
40. Vogt, J.V.; Safriel, U.; Von Maltitz, G.; Sokona, Y.; Zougmore, R.; Bastin, G.; Hill, J. Monitoring and assessment of land degradation and desertification: Towards new conceptual and integrated approaches. *Land Degrad. Dev.* **2011**, *22*, 150–165. [CrossRef]
41. Mendas, A.; Delali, A. Integration of multi-criteria decision analysis in GIS to develop land suitability for agriculture: Application to durum wheat cultivation in the region of Mleta in Algeria. *Comput. Electron. Agric.* **2012**, *83*, 117–126. [CrossRef]
42. Harris, S.; McDowell, R.; Lilburne, L.; Laurenson, S.; Dowling, L.; Guo, J.; Pletnyakov, P.; Beare, M.; Palmer, D. Developing an indicator of productive potential to assess land use suitability in New Zealand. *Environ. Sustain. Indic.* **2021**, *11*, 100128. [CrossRef]
43. Alturk, B.; Kurc, H.C.; Konukcu, F.; Kocaman, I. Multi-criteria land use suitability analysis for the spatial distribution of cattle farming under land use change modeling scenarios in Thrace Region, Turkey. *Comput. Electron. Agric.* **2022**, *198*, 107063. [CrossRef]
44. United Nations Department of Economic and Social Affairs (UN DESA). *The Sustainable Development Goals Report 2024*; UN DESA: New York, NY, USA, 2024. Available online: https://unstats.un.org/sdgs/report/2024/ (accessed on 18 June 2025).
45. Alhamad, M. Ecological and species diversity of arid Mediterranean grazing land vegetation. *J. Arid. Environ.* **2006**, *66*, 698–715. [CrossRef]
46. Al-Bilbisi, H. Topography and morphology. In *Atlas of Jordan: History, Territories and Society*; Ababsa, M., Ed.; Presses de l'Ifpo: Beyrouth, Lebanon, 2013; pp. 42–46. Available online: http://books.openedition.org/ifpo/4859 (accessed on 5 April 2025).
47. Environmental Systems Research Institute (ESRI). *ArcGIS Pro, Version 3.3*; ESRI: Redlands, CA, USA, 2024.
48. Susha Lekshmi, S.U.; Singh, D.; Shojaei Baghini, M. A critical review of soil moisture measurement. *Measurement* **2014**, *54*, 92–105. [CrossRef]
49. Tang, H.; Li, Q.; Bao, Q.; Tang, B.; Li, K.; Ding, Y.; Luo, X.; Zeng, Q.; Liu, S.; Shu, X.; et al. Interplay of soil characteristics and arbuscular mycorrhizal fungi diversity in alpine wetland restoration and carbon stabilization. *Front. Microbiol.* **2024**, *15*, 1376418. [CrossRef]
50. Ameer, S.; Ibrahim, H.; Kulsoom, F.N.U.; Ameer, G.; Sher, M. Real-time detection and measurements of nitrogen, phosphorous and potassium from soil samples: A comprehensive review. *J. Soils Sediments* **2024**, *24*, 2565–2583. [CrossRef]
51. Nelson, D.W.; Sommers, L.E. Total carbon, organic carbon, and organic matter. In *Methods of Soil Analysis, Part 3—Chemical Methods*; Sparks, D.L., Ed.; SSSA Book Series No. 5; Soil Science Society of America: Madison, WI, USA, 1996; pp. 961–1010.
52. Robinson, D.A.; Thomas, A.; Reinsch, S.; Lebron, I.; Feeney, C.J.; Maskell, L.C.; Wood, C.M.; Seaton, F.M.; Emmett, B.A.; Cosby, B.J. Analytical modelling of soil porosity and bulk density across the soil organic matter and land-use continuum. *Sci. Rep.* **2022**, *12*, 11099. [CrossRef]
53. Alonso, L. Forage biomass estimated with a pre-calibrated equation of a rising platemeter in pastures grown in tropical conditions. *Grasses* **2023**, *2*, 127–141. [CrossRef]
54. Qader, S.H.; Utazi, C.E.; Priyatikanto, R.; Najmaddin, P.; Hama-Ali, E.O.; Khwarahm, N.R.; Tatem, A.J.; Dash, J. Exploring the use of Sentinel-2 datasets and environmental variables to model wheat crop yield in smallholder arid and semi-arid farming systems. *Sci. Total Environ.* **2023**, *869*, 161716. [CrossRef] [PubMed]
55. Tempa, K.; Ilunga, M.; Agarwal, A. Utilizing Sentinel-2 satellite imagery for LULC and NDVI change dynamics for Gelephu, Bhutan. *Appl. Sci.* **2023**, *14*, 1578. [CrossRef]

56. Harmse, C.J.; Gerber, H.; Van Niekerk, A. Evaluating several vegetation indices derived from Sentinel-2 imagery for quantifying localized overgrazing in a semi-arid region of South Africa. *Remote Sens.* **2022**, *14*, 1720. [CrossRef]
57. Main-Knorn, M.; Pflug, B.; Louis, J.; Debaecker, V.; Müller-Wilm, U.; Gascon, F. Sen2Cor for Sentinel-2. In *Image and Signal Processing for Remote Sensing XXIII.*; Bruzzone, L., Ed.; SPIE: Bellingham, WA, USA, 2017; Volume 10427, p. 1042704. [CrossRef]
58. Mohammad, A. The effect of slope aspect on soil and vegetation characteristics in Southern West Bank. *Bethlehem Univ. J.* **2008**, *27*, 9–25.
59. Fadl, M.A.; Al-Yasi, H.M.; Alsherif, E.A. Impact of elevation and slope aspect on floristic composition in Wadi Elkor, Sarawat Mountain, Saudi Arabia. *Sci. Rep.* **2021**, *11*, 16160. [CrossRef]
60. García-Gamero, V.; Peña, A.; Laguna, A.; Giráldez, J.; Vanwalleghem, T. Factors controlling the asymmetry of soil moisture and vegetation dynamics in a hilly Mediterranean catchment. *J. Hydrol.* **2021**, *598*, 126207. [CrossRef]
61. Yang, Y.; Chen, C.; Liu, J.; Liu, Y.; Luo, J.; Liu, J.; Zhang, Y. Remote sensing-based estimation of forage yield and quality: A review of models, methods, and sensors. *Remote Sens.* **2023**, *15*, 1600. [CrossRef]
62. Food and Agriculture Organization (FAO). *Guidelines: Land Evaluation for Extensive Grazing*; Soil Bulletin No. 58; FAO: Rome, Italy, 1991. Available online: https://www.fao.org/4/t0412e/t0412e.pdf (accessed on 10 May 2025).
63. Rahman, M.M.; Szabó, G. Sustainable urban land-use optimization using GIS-based multicriteria decision-making (GIS-MCDM) approach. *ISPRS Int. J. Geo-Inf.* **2022**, *11*, 313. [CrossRef]
64. Al-Awadhi, T.; Al Ramimi, W.; Al Jabri, K.; Abulibdeh, A. Solar farms suitability analysis using GIS-based Analytic Hierarchy Process (AHP) multi-criteria: A case study of Al Duqm, Oman. *Renew. Energy* **2025**, *241*, 122295. [CrossRef]
65. Al-Hamad, A.A.; Al-Taani, A.A.; Ghrefat, H.; Khawajah, M.; Zoubi, A. Assessment of heavy metals in greenhouse cultivated soils, Northern Jordan. *Pol. J. Environ. Stud.* **2024**, *33*, 61–75. [CrossRef] [PubMed]
66. El-Radaideh, N.M.; Al-Taani, A.A.A.K. Geo-environmental study of heavy metals of the agricultural highway soils, NW Jordan. *Arab. J. Geosci.* **2018**, *11*, 787. [CrossRef]
67. Assiri, M.E.; Ali, M.A.; Alamri, L.; Siddiqui, M.H.; Ghulam, A.S.; Shahid, S. Spatio-temporal dynamics of vegetation and land surface temperature in Saudi Arabia: Impacts of climate change on agricultural sites from 2010 to 2023. *Int. J. Climatol.* **2025**, *45*, e8781. [CrossRef]
68. Rababa'a, G.; Al-Bakri, J. Mapping land cover in the Dead Sea Basin from Landsat TM satellite imagery. *Dirasat Pure Sci.* **2006**, *33*, 189–203.
69. HERD. *Healthy Ecosystems for Rangeland Development (HERD) Project*; Ministry of Environment, Jordan & IUCN: Amman, Jordan, 2023. Available online: https://jo.test.chm-cbd.net/projects/healthy-ecosystems-rangeland-development-herd (accessed on 20 September 2025).
70. Muhaidat, R.; Al-Qudah, K.; Al-Taani, A.A.; AlJammal, S. Assessment of nitrate and nitrite levels in treated wastewater, soil, and vegetable crops at the upper reach of Zarqa River in Jordan. *Environ. Monit. Assess.* **2019**, *191*, 153. [CrossRef]
71. Akhzari, D.; Pessarakli, M.; Eftekhari Ahandani, S. Effects of grazing intensity on soil and vegetation properties in a Mediterranean rangeland. *Commun. Soil Sci. Plant Anal.* **2015**, *42*, 2814–2828. [CrossRef]
72. Jawasreh, K.; Alqaisi, O.; Alsatary, Y.; Al-Nsoor, A. Grazing behavior of Awassi sheep and the biodiversity of plant species under semi-arid reserved conditions. *Arid. Ecosyst.* **2012**, *2*, 245–252. [CrossRef]

Disclaimer/Publisher's Note: The statements, opinions and data contained in all publications are solely those of the individual author(s) and contributor(s) and not of MDPI and/or the editor(s). MDPI and/or the editor(s) disclaim responsibility for any injury to people or property resulting from any ideas, methods, instructions or products referred to in the content.